Measured Orientation and Internal Stress Distributions in Melt-Spun Fibers

W. PAUL BELL* and DAN D. EDIE,† *Department of Chemical Engineering, Clemson University, Clemson, South Carolina 29634-0909*

Synopsis

In this investigation, experimentally measured radial birefringence profiles are compared to internal stress distributions as predicted by a mathematical model. A direct indicator of the degree of molecular orientation, fiber birefringence, is found to correlate well with the stress distributions as calculated from radial temperature variations. In an initial study of glass fibers, no radial birefringence profiles are found, indicating that any residual stresses present are small. In polystyrene fibers, however, large radial variations in birefringence are observed and are shown to be directly related to the calculated internal stresses.

INTRODUCTION

One of the most important phenomena which occurs during the melt spinning of fibers is the development of molecular orientation within the fiber. Synthetic fibers are most commonly spun from polymeric materials composed of long-chain molecules which are randomly coiled in a stress-free state. When, as in melt spinning, a unidirectional stress is applied to a polymer melt, the chains uncoil and preferentially align in the direction of the stress. This molecular orientation is "frozen in" when the temperature of the polymer melt is reduced to a point below the material's glass transition. In this state, molecular motion is severely restricted and the oriented polymer chains cannot easily return to the lower energy coiled state. In a melt-spun fiber, molecular orientation can be detected by x-ray diffraction techniques, but birefringence, an optical property, is by far the best indicator of the degree of molecular orientation for an amorphous fiber.

Elongational flow has been firmly established as the primary cause of molecular orientation during melt spinning.[1] Some workers have proposed that shear flow in the spinneret orients the polymer molecules but most of this orientation is quickly relieved due to the high temperature in this region. However, velocity gradients in the spinline cannot explain the development of a radial variation in orientation observed in many fibers, especially at high take-up speeds. Axial velocity gradients do not vary significantly across the fiber radius, especially near the solidification point where diameter reduction is essentially complete. Yet "skin-core" differentiation of orientation and structure is clearly seen in many fibers. Ziabicki and Kawai[1] propose radial

* Present address: Tennessee Eastman Company, Kingsport, Tennessee.
† To whom correspondence should be addressed.

Journal of Applied Polymer Science, Vol. 33, 1089–1102 (1987)

CCC 0021-8995/87/041089-14$04.00

temperature variation as the cause of this structure. Center-to-surface temperature differences in the spinline, estimated to be as large as 15°C, result in considerable variation in physical, mechanical, and rheological properties across the fiber radius. Viscosities of the center and surface layers of the fiber may differ by as much as 40%. Since the fiber behaves much as a solid in this region, the axial velocity of the center and surface layers must be the same. Therefore the axial stress at the surface must be greater than that in the interior. Such variation of stress may cause this radial variation in orientation which is "frozen in" when the fiber passes through the glass transition.

In an earlier work,[2] the authors present a mathematical model which determines internal stress distributions in a melt-spun fiber assuming the material behaves as a linearly elastic solid. Stress profiles near the solidification point are found to be similar to those predicted by Ziabicki and Kawai.[1] The current work involves comparison of calculated stress profiles with experimentally measured radial variations in orientation. The objective of this investigation is to determine whether or not a valid relationship between radial temperature gradients and orientation in melt-spun fibers exists. Experimentally, this requires the measurement of radial birefringence profiles in actual fibers. Such measurements are difficult and some explanation of the technique involved is necessary.

BIREFRINGENCE IN FIBERS

A material is termed "birefringent" if the speed of light in the material depends on the polarization of the light. Quartz is a common example of a

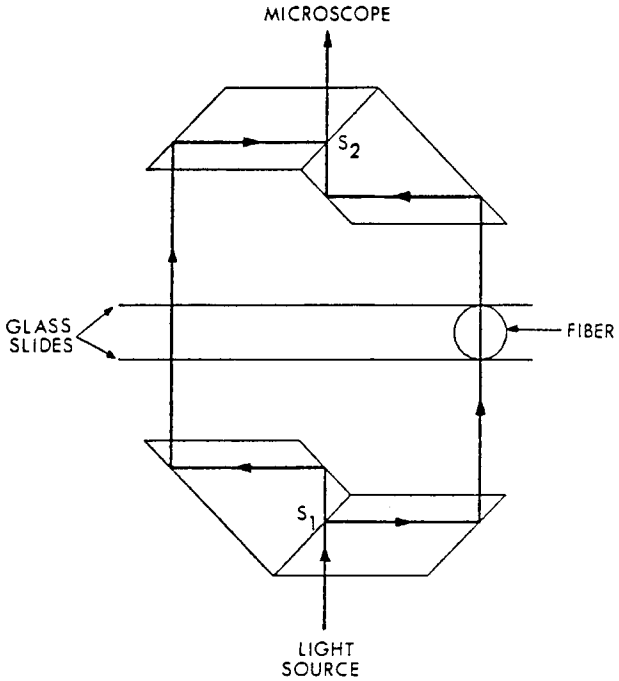

Fig. 1. Light path in a double-beam interference microscope.

birefringent material. A quartz crystal has an optic axis along which the refractive index is a maximum and perpendicular to which the index is a minimum. Birefringence Δn is defined as

$$\Delta n = n_{11} - n_{\perp} \tag{1}$$

where n_{11} and $n_{\perp}$ are the refractive indices parallel and perpendicular to the optic axis, respectively. For fibers, the optic axis is arbitrarily defined as the fiber axis.

Birefringence Measurement

Many methods exist for the measurement of birefringence in fibers. The simpler techniques, such as the Becke line method[3] and the fiber refractometer,[4] determine the two refractive indices separately by a trial-and-error process. Compensatory techniques,[5] on the other hand, measure fiber birefringence directly by interferometry. Such measurements represent a significant improvement over the other methods, since birefringence is determined from measurable optical path differences and the laws of physics. Multiple beam interferometry further improves on compensatory techniques by providing for determination of the individual indices.[6]

The double-beam interference microscope[7,8] shown in Figure 1 is similar to the multiple beam interferometer. At S_1, a monochromatic polarized beam of light is split into two beams, one of which passes unretarded to S_2. The other beam passes through the fiber and is retarded by the difference in refractive indices of the fiber and the immersion liquid. This beam then passes to S_2, where it is recombined with the first beam and enters the microscope. This generates an interference pattern similar to that in Figure 2, from which the refractive index is calculated as

$$n_a = n_L + \frac{d\lambda}{Dt} \tag{2}$$

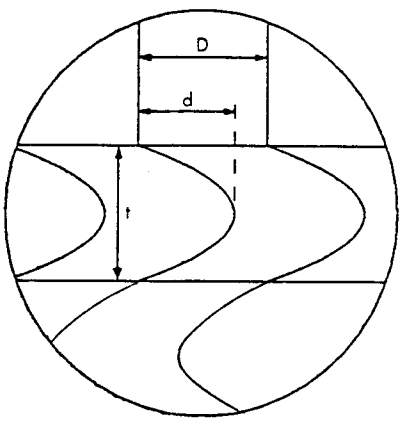

Fig. 2. Typical interference pattern obtained from a fiber using an interference microscope.

Radial Variation of Birefringence

One important bit of information is available from interference techniques which the other methods of birefringence measurement cannot provide—radial variation of birefringence. As can be seen in Figure 2, the displacement of the interference fringe by the fiber varies with radial distance from the fiber axis. This is due in part to the fact that the fiber is not as thick at these points, but it may also be caused by a radial variation of the refractive index.[7] Roche and Davis[8] present a method for interpreting double-beam interference patterns to determine the radial birefringence profile. The fiber is first idealized as a series of N concentric shells, each with a constant refractive index, as in Figure 3. If the displacement d is measured for N radial positions r, then the chord-averaged refractive index $n(r)$ is given by

$$n(r) = n_L + \frac{d(r)}{t(r)} \frac{\lambda}{D} \tag{3}$$

If the fiber is assumd to be cylindrical with an outside radius R, then $t(r)$ is a simple geometric quantity given by

$$t(r) = 2(R^2 - r^2)^{0.5} \tag{4}$$

The chord-averaged index is defined as

$$n(r)t(r) = \sum_{j=1}^{N} n_j l_j(r) \tag{5}$$

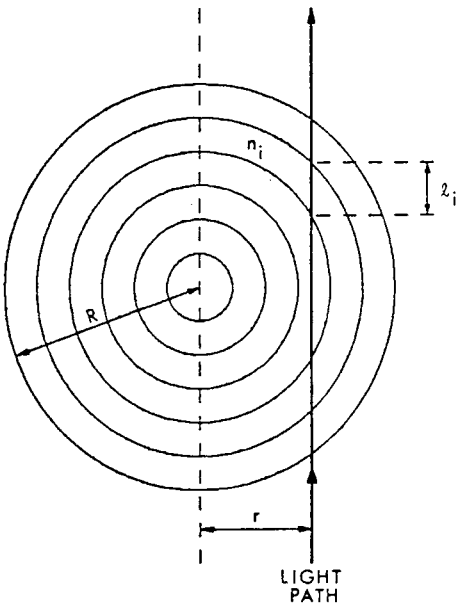

Fig. 3. Shell model used for determining radial birefringence profiles.

where n_j is the refractive index of shell j and $l_j(r)$ is the distance the light beam must travel through shell j at r. When Eq. (5) is written for N values of r, the system of equations may be solved for the shell indices n_j. Obviously, the accuracy of this technique is limited by the accuracy of the fringe displacement measurements. It is also possible that the shell model will not adequately represent rapid changes in birefringence observed near the surface of some fibers. For these reasons, Roche and Davis recommend that surface data be obtained by extrapolation.[8]

A more rigorous method involves assuming a functional form for the refractive index profile. If, for example, a polynomial of degree N is assumed, the discontinuity problems of the shell model are eliminated. Thus, the refractive index profile $n^*(r)$ is given by

$$n^*(r) = \sum_{j=0}^{N} a_j r^j \tag{6}$$

Using the coordinate system in Figure 4, Eq. (5) is replaced by

$$2n(z)L = \int_{-L}^{L} n^*(r)\, dl \tag{7}$$

where z is the distance from the center of the fiber. If $N = 3$ is used, the integral in Eq. (7) can be evaluated to give

$$n(z)L = a_0 L + \frac{a_1}{2}\left[RL + z^2 \ln\left(\frac{L+R}{z}\right)\right] + a_2\left[\frac{L^3}{3} + z^2 L\right] + \frac{a_4}{4}\left[LR^3 + \frac{3z^2 LR}{2} + \frac{3z^4}{2}\ln\left(\frac{L+R}{z}\right)\right] \tag{8}$$

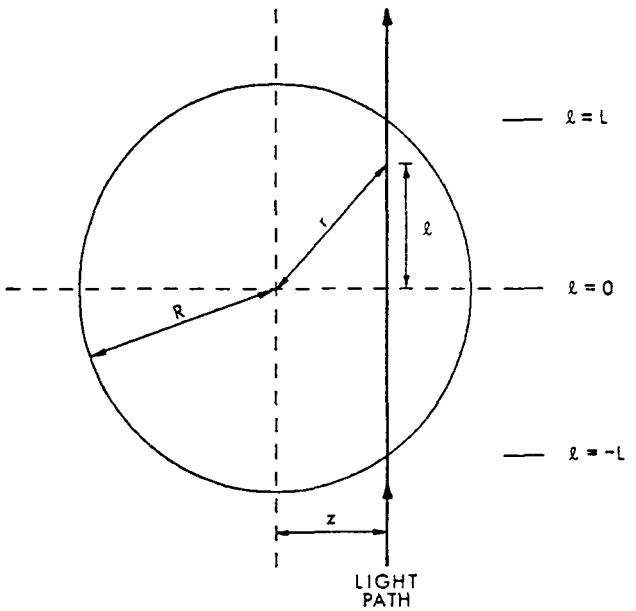

Fig. 4. Continuous model used for determining radial birefringence profiles.

If Eq. (8) is written for four values of z, the resulting system of equations may be solved directly for the coefficients a_j. Alternatively, measurements may be made at more than four points and a multivariable least-squares technique used to determine the "best" coefficients. This has the advantage of reducing some of the error which may be introduced in measuring the fringe displacements. This more rigorous method employing a least-squares technique was used in the present work.

PLAN OF EXPERIMENTATION

Determining the relationship between internal stresses and molecular orientation in melt-spun fibers requires a combination of experimental measurement of birefringence and theoretical prediction of stresses. Fibers must be spun at known conditions and the radial variation of birefringence in each determined by the techniques described in the previous section. A model of stress development[2] must then be applied to predict the internal stresses present in these fibers during spinning. The results of these two procedures may then be compared to see if any correlation exists.

Glass Fibers

A preliminary investigation of stresses and orientation in glass fibers was conducted. Using the model of Bell and Edie,[2] internal stress distributions of fibers were first calculated. As shown in Figure 5, the axial stress at the surface is increasing near the solidification point, and approaches the spinline tension as z increases. Radial and hoop stresses, however, decay to zero values as z increases, as shown in Figures 6 and 7. Since glass molecules do not orient under stress, the internal stresses should result in no "frozen-in" birefringence in the fibers.

Glass fibers spun under controlled conditions were obtained for measurement of birefringence profiles. When properly mounted and placed in a double-beam interference microscope, interference patterns similar to that in

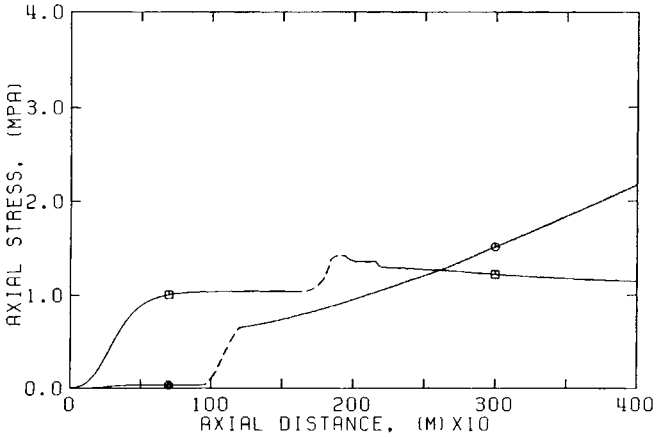

Fig. 5. Calculated profiles of axial stress for polystyrene and glass fibers: (⊡) Polystyrene; (⊙) Glass.

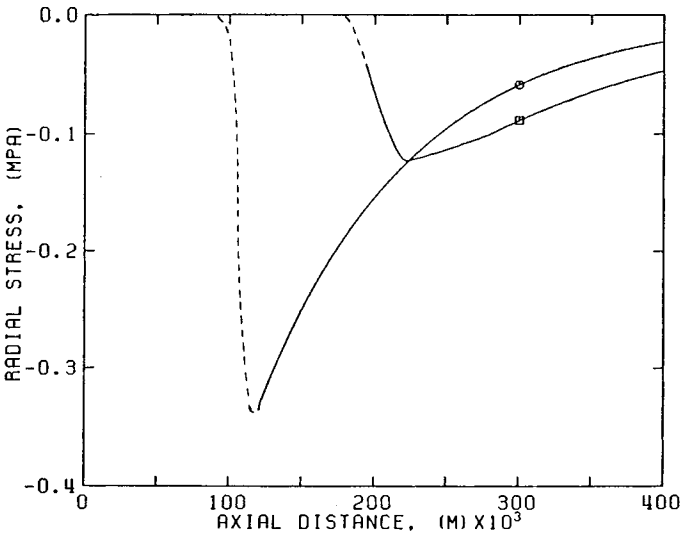

Fig. 6. Calculated profiles of radial stress for polystyrene and glass fibers: (⊡) Polystyrene; (⊙) Glass.

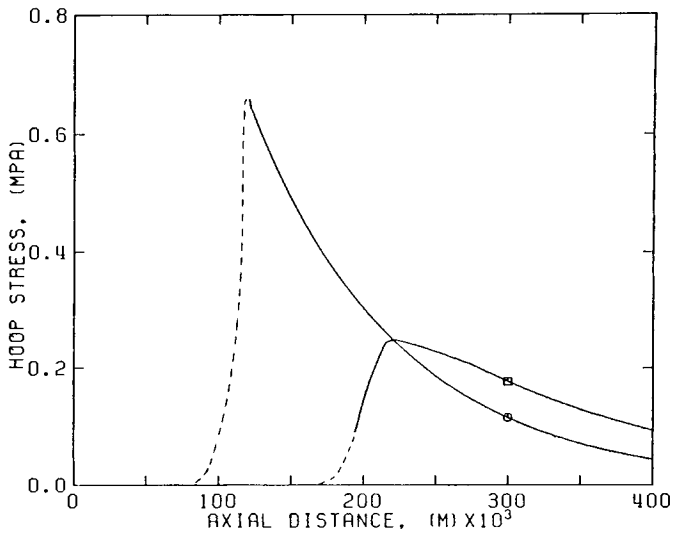

Fig. 7. Calculated profiles of hoop stress for polystyrene and glass fibers: (⊡) Polystyrene; (⊙) Glass.

Figure 2 were obtained for each polarization of the incident light. The fringes were not sharply defined, due to the fact that the light source of the microscope was not truly monochromatic. This made measurement of the required fringe displacement data difficult. In addition, fiber diameters varied slightly from one sample to the next. For these reasons, multiple measurements were made and average values determined.

As shown in Figure 8, the measured birefringence profiles vary noticeably from one sample to the next. The primary cause of this variation is error in

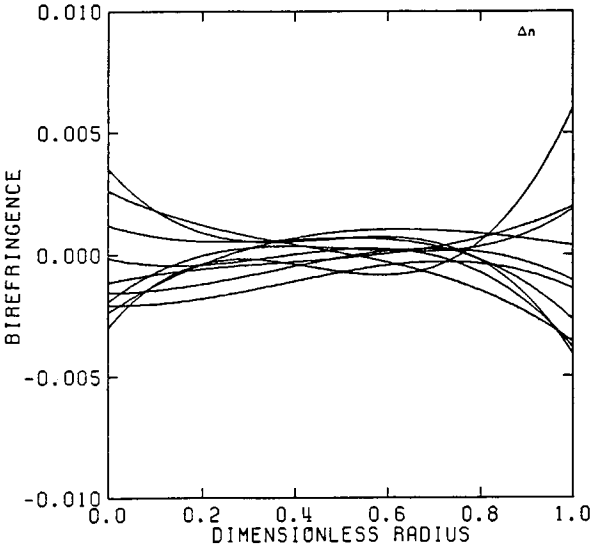

Fig. 8. Measured birefringence profiles of glass fibers.

manually measuring the fringe displacements, indicating that some automated procedure may be more reliable. When the profiles are averaged, radial variations essentially disappear, with a center-to-center surface difference of only 0.00015. Considering the variations observed among the individual fibers, this radial variation is negligibly small. Thus, the glass fibers have no measurable birefringence, implying that the fibers are not oriented and residual stresses, if they do indeed exist, are small.

Although this work led to no definite conclusions regarding internal stresses and orientation, it did help in refining the experimental technique. Three problems were discovered and corrected. First, it was found that multiple measurements were needed to ensure that diameter variations do not affect the results. Second, as noted above, fringe displacements had to be measured carefully to ensure accuracy. Finally, problems were found in determining the profiles near the center and surface of the fiber. At the center, this is caused by measurement errors, since the fringes are poorly defined in this region. Surface errors, however, are due to refraction of light. Roche and Davis[8] note this problem and suggest several methods of reducing this error. Fortunately, it was found that averaging the profiles of several fibers tends to eliminate most of these errors.

Polystyrene Fibers

Unlike glass fibers, polystyrene fibers orient under stress, so an investigation should yield some valuable information. Polystyrene fibers were spun in the laboratory under several sets of spinning conditions, as noted in Table I. When the refractive index and birefringence profiles of these fibers were measured, the profiles varied among the individual samples, as with the glass fibers. The averaged birefringence profiles for each of the six runs are presented in Figure 9.

TABLE I
Run Conditions for Polystyrene Fiber Production

Run number	Spinning temperature (K)	Ambient air temperature (K)	Spinneret diameter (m) $\times 10^6$	Mass flow rate (kg/s) $\times 10^6$	Take-up speed (m/s)
1	538.15	300.95	688.8	3.573	2.6175
2	538.15	300.95	688.8	4.955	2.6175
3	538.15	300.95	688.8	8.530	2.6175
4	538.15	300.95	688.8	10.640	2.6175
5	538.15	293.15	688.8	5.110	2.5784
6	538.15	293.15	688.8	11.920	2.5784

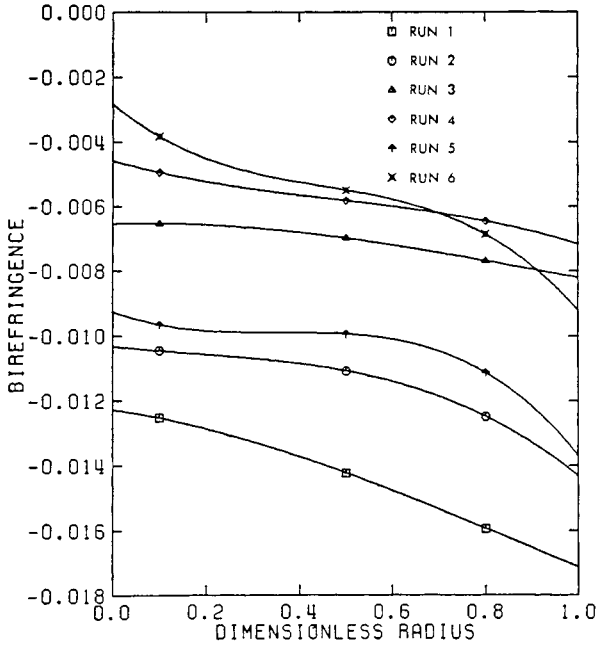

Fig. 9. Measured birefringence profiles of polystyrene fibers.

The profiles in Figure 9 lead to several observations. First, the level of birefringence decreases as mass flow rate increases (Runs 1 through 4). Since increasing W decreases the draw ratio and hence elongation rates, this is the expected effect. Differential birefringence, the difference between the birefringence at the center of the fiber and that at the surface, also decreases as mass flow rate increases. Decreasing ambient air temperature (from Run 2 to Run 5 and from Run 4 to Run 6) decreases the level of birefringence, a finding contrary to the predictions of the authors' model.[2] Differential birefringence, on the other hand, increases as T_a decreases. It must be noted here that ambient air temperature is not the only difference between Runs 2 and 5 and Runs 4 and 6; take-up speed and mass flow rate also change slightly. These factors will later be shown to explain the apparent anomaly in the results.

TABLE II
Summary of Simulation Results for Polystyrene Fibers

Run number	Winder force (N) $\times 10^4$	Spinline tension (MPa)	Max. radial temp. diff. (K)	Radial temp. diff. at sol. (K)	Sol. point (m) $\times 10^3$	Max. σ_{rr} at center (MPa)	Max $\sigma_{\theta\theta}$ at surface (MPa)
1	11.854	0.903	7.49	3.07	131.1	−0.104	0.210
2	12.071	0.663	7.93	3.26	171.8	−0.110	0.221
3	12.341	0.394	8.71	3.60	269.6	−0.121	0.245
4	12.410	0.318	9.06	3.67	323.7	−0.119	0.254
5	12.395	0.650	8.21	3.59	167.6	−0.125	0.252
6	12.744	0.287	9.53	4.15	338.2	−0.138	0.291

Stress Calculations

At this point, the stress development model[2] is applied using the conditions listed in Table I. The results of these simulations are summarized in Table II. As expected, spinline tension decreases with increasing mass flow rate (Runs 1 through 4), which explains the observed decrease in birefringence. The maxima in radial and hoop stresses generally increase as W increases, since the radial temperature gradients in the fiber increase. The spinline tension in Run 5 is less than that in Run 2, and Runs 4 and 6 compare similarly. Apparently, the change in T_a increases the winder force only slightly, while changing mass flow and take-up speed increases the final fiber diameter to a greater degree. The net effect of this is a decrease in the spinline tension. Thus the observed decrease in birefringence in Runs 5 and 6 is explained. Finally, the decrease in T_a increases the maximum radial and hoop stresses.

Internal Stresses vs. Orientation

Ziabicki and Kawai[1] found that at low take-up speeds (less than 2000 m/min), the average birefringence of a fiber is directly proportional to the spinline tension, or

$$\overline{\Delta n} = C_s(\sigma_{zz} - \sigma_{rr}). \tag{9}$$

This relationship has been observed in many materials and forms the basis of stress-optical theory.[9] Figure 10 shows the measured diameter-averaged birefringence values plotted against calculated spinline tensions for each of the experimental runs. When a linear least-squares routine is applied to the data, the line in the figure is found. The corresponding stress-optical coefficient is -16.71 Br (1 Br = 10^{-9} Pa^{-1}).

Many factors influence the determination of a stress-optical coefficient from the data of Figure 10. Foremost is experimental error in the measurement of the birefringence values. As noted earlier, the measurements are difficult and are subject to operator bias. Experimental error may also be present in the data in Table I. Precise control of the laboratory spinning operation is limited, so the true spinning conditions may be slightly different from those listed. Finally, the effects of inertia, air drag, and gravity, which are neglected in calculating the spinline tension, may be greater than originally thought. This

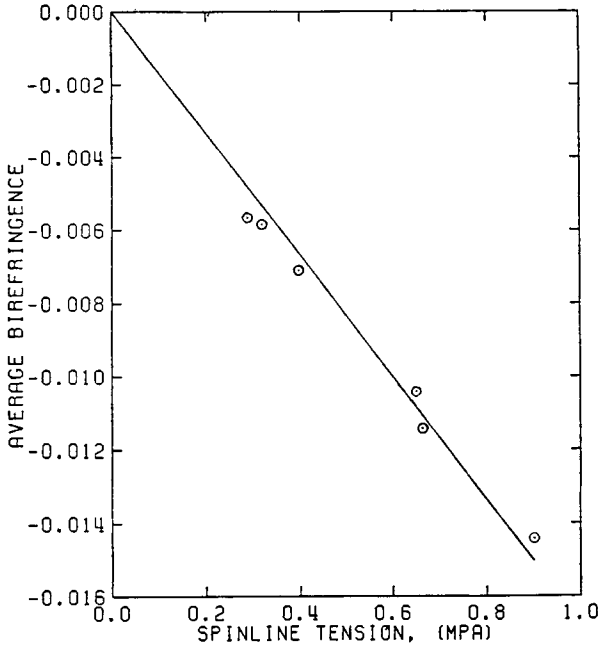

Fig. 10. Determination of stress-optical coefficient for polystyrene fibers.

may be particularly true at high take-up speeds. These factors may explain why the stress-optical coefficient determined here differs from literature values. It must also be noted that the literature values also vary widely (-6.1 to $+6.5$ Br).[9,10]

Using the experimentally determined stress-optical coefficient, the birefringence profiles in Figure 9 can be converted into stress profiles by Eq. (9). These "measured" profiles of the stress difference $\Delta\sigma$ are then plotted with the calculated profiles at the solidification point. Figure 11 shows the results from Run 1. Good agreement between the measured and calculated stress profiles is found. The trends are the same, as are the orders of magnitude. In general, the calculated stress profiles show greater radial variation than the measured profiles. This difference may be due to the fact that stress-relaxation is not included in the calculations. If some relaxation has occurred in the fibers, then the radial variations of stress should be decreased from what it was originally. When the data are plotted as measured versus calculated stress differences, Figure 12 results. Although the agreement is not perfect, the scatter of data about the 45° line is fairly even. In view of the fact that stress–relaxation effects have been neglected, these results indicate that there is indeed a valid relationship between the calculated internal stresses and orientation in melt-spun fibers.

Again, there are many potential sources of error which may account for the deviation of the results of this study. The factors discussed relative to determining the stress-optical coefficient have similar effects here. Additionally, the calculated stress profiles shown in the figures are not those at the exact solidification point. As noted in the earlier article,[2] numerical instabilities prevent accurate prediction of the stresses in this area. At approximately

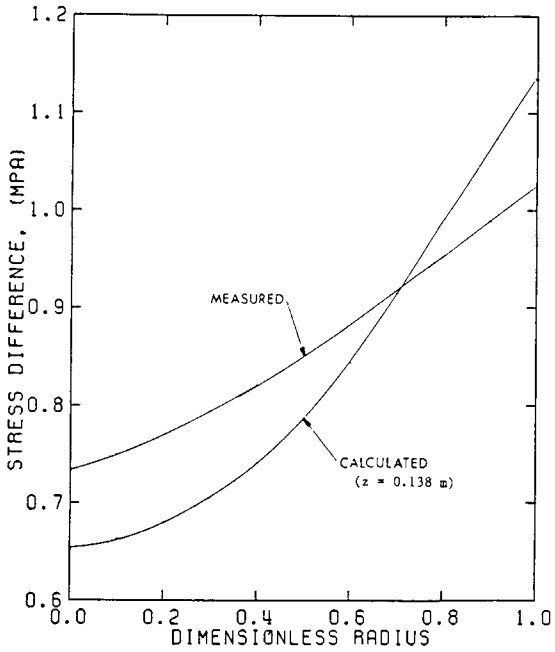

Fig. 11. Comparison of measured and predicted stress difference profiles for polystyrene fibers (Run 1).

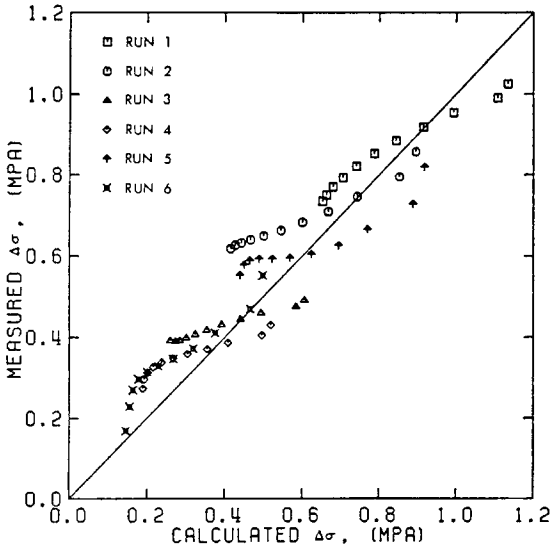

Fig. 12. Comparison of measured and predicted stress difference for polystyrene fibers.

0.010 m below the solidification point, the finite element calculations are again stable; the profiles at this point are those used in the above discussion. Even with these potential errors, the relationship between internal stresses and orientation is obvious.

Earlier Ziabicki and Kawai[1] showed a similar result by viewing the fiber as a viscous liquid. The viscosity of the material varies across the fiber radius

due to temperature variation. Since the velocity must be constant at the solidification point, axial stress must vary. In the present work, the fiber is modeled as an elastic solid. Axial strain is constant across the radius; stress varies because modulus is not constant. Either model may be valid, but one would think that the properties of the material near the solidification point are more solidlike. The Deborah number is an indicator of the relative importance of the viscous and elastic effects in the material. Defined as the ratio of the material's characteristic time to the time scale of the experiment, the Deborah number De becomes for a melt-spun fiber

$$\mathrm{De} = \tau \frac{dv_z}{dZ} \tag{10}$$

Ziabicki and Kawai[1] estimate the relaxation time as

$$\tau = \frac{\beta}{E} \tag{11}$$

At the solidification point, the elongation rate is relatively small (0.01 s^{-1} or less), since drawdown of the fiber is essentially complete at this point. The elongational viscosity, however, is very large; for polystyrene, it is 1.22×10^8 Pa · s at the glass transition, using the relationship from Bell and Edie.[2] The modulus is small at this point, but it has a finite value. Taking E as 3.0×10^5 Pa for polystyrene at the glass transition, the estimated Deborah number is roughly 4. A Deborah number greater than unity indicates elastic behavior dominates at the solidification point. At a distance of 0.010 m from the spinneret, the temperature is 530 K and the elongation rate is 52 s^{-1}. The corresponding Deborah number is roughly 0.2, using the modulus value assumed above. Thus, modeling the material as a viscous liquid is valid near the spinneret, but modeling as an elastic solid is much more appropriate in the solidification zone.

SUMMARY

Orientation develops in a melt-spun fiber due to the deformation process during fiber formation. At low take-up speeds, the degree of orientation, as evidenced by the fiber's birefringence, is directly related to the spinline tension. Radial temperature variations have been shown to result in radial variations in orientation. By modeling the fiber as an elastic solid, these temperature gradients have been related to internal thermal stresses in the fiber. Thus, a relationship between internal stress and radial orientation gradients has been established.

APPENDIX: NOMENCLATURE

a_j Coefficient in polynomial expansion
C_s Stress-optical coefficient (Br)
d Fringe displacement (m)
D Fringe-to-fringe distance (m)
De Deborah number
E Elastic modulus (Pa)
l_j Length of light path in shell j (m)

L Length of light path through fiber (m)
n_a Average refractive index
n_j Refractive index of shell j
n_L Refractive index of immersion liquid
n_{11} Refractive index parallel to optic axis
$n_\perp$ Refractive index perpendicular to optic axis
R Radius of fiber (m)
t Thickness of fiber (m)
v_z Axial velocity (m/s)
z Distance from center of fiber (m)
Z Distance from spinneret (m)
β Elongational viscosity (Pa · s)
Δn Birefringence
λ Wavelength of light (m)
σ_{zz} Normal axial stress (Pa)
σ_{rr} Normal radial stress (Pa)
$\sigma_{\theta\theta}$ Tangential (hoop) stress (Pa)
τ Relaxation time (s)

References

1. A. Ziabicki and H. Kawai (eds.), *High Speed Fiber Spinning*, Wiley, New York, 1985.
2. W. P. Bell and D. D. Edie, *J. Applied Polym. Sci.*, **4**, 771 (1987).
3. A. N. J. Heyn, *Textile Res. J.*, **22**, 513 (1952).
4. W. E. Morton and J. W. S. Hearle, *Physical Properties of Textile Fibers*, Heinemann, London, 1975.
5. R. C. Faust, *Proc. Phys. Soc. London*, **B67**, 138 (1954).
6. A. A. Hamza and H. I. Adb El-Kader, *Textile Res. J.*, **53**, 205 (1983).
7. J. H. McLean, *Textile Res. J.*, **35**, 242 (1965).
8. E. J. Roche and H. A. Davis, *Proc. Fiber Prod. Conf. 1983*, 3-1 (1983).
9. H. Janeschitz-Kriegl, *Polymer Melt Rheology and Flow Birefringence*, Springer-Verlag, New York, 1983.
10. R. H. Boundy (ed.), *Styrene, Its Polymers, Copolymers, and Derivatives*, Reinhold, New York, 1952.

Received July 2, 1986
Accepted July 8, 1986